ROZPRAWY INŻYNIERSKIE • ENGINEERING TRANSACTIONS • 24, 4, 771–786, 1976
Polska Akademia Nauk • Instytut Podstawowych Problemów Techniki

PHYSICALLY AND GEOMETRICALLY NONLINEAR ANALYSIS OF STRUCTURES USING ONE- AND TWO-DIMENSIONAL FINITE ELEMENTS

K. DEMS (ŁÓDŹ) and M. KLEIBER (WARSZAWA) (*)

The paper deals with the application of the finite element method for large elasto-plastic deformation analysis. The fundamental system of equations in Eulerian description has been obtained from the very general variational theorem. The geometric stiffness matrices have been derived for geometric nonlinear, one- and two-dimensional problems. The computer program, which have been based on the ASKA program package, has also been discussed. The paper is illustrated by the numerical examples.

1. INTRODUCTION

The analysis of various structural problems in the both geometrically and physically nonlinear range of deformations has been a subject of considerable interest for almost a decade starting with papers of FELIPPA [1], LEVINE et al. [6], MARCAL [2], STRICKLIN et al. [5], YAGHAMI [3], HABBITT et al. [4]. All these papers, as well as almost all of many others which have appeared later, were based on the finite element method reducing the solution of a problem to that of tracing a nonlinear load-displacement path by solving a system of nonlinear algebraic equations.

With the variety of numerical procedures naturally comes the question of which technique is best suited for a particular application. At present we witness the situation that while there exist very many procedures to solve nonlinear problems within the finite element concept, there is only small experience suggesting which of them are to be used for a specific application. This is why all numerical procedures and comparisons involving the both nonlinearity sources are likely to be very useful for further development of the method.

The present paper explores the problem formulation (via a variational principle of the one-field type) for large elastic-plastic deformation analysis. The approach is demonstrated by determining geometric stiffness matrices for truss and triangular plane stress elements. The comparison of the geometric stiffness matrix for simple truss member with that derived in [8] within the "natural" discretized approach shows the strict equivalence of the two formulations. In the paper solutions are presented for highly nonlinear truss and plane stress problem.

(*) DAAD (K. Dems) and Humboldt Foundation (M. Kleiber) scholars on leave of absence from the Technical University, Łódź, Poland (K.D.) and the Institute of Fundamental Technological Research, Polish Academy of Sciences, Warsaw, Poland (M.K.).

Basically, two different approaches have been pursued in incremental nonlinear finite element analysis. In the first, static and kinematic variables are referred to an updated configuration in each load step. This procedure is generally called Eulerian, moving coordinates or updated formulation. In the second approach, which is generally called the Lagrangian formulation, all static and kinematic variables are referred to the initial configuration.

It is believed that in the case of significant nonlinearities which exist usually in structures made of pinjointed bars the Eulerian method is more efficient. Moreever, as plasticity relations are normally written using the actual (true) quantities, the updated formulation has been chosen to analyse the elastic-plastic behaviour of structures.

2. Basic equations

The fundamental system of equations we shall obtain from the very general continuum mechanics variational theorem which, for the incremental deformation process described with regard to the actual configuration, can be stated as follows [7]: At a given time t, when the state of the elastic-plastic continuum is described by the field of displacement u_i, the Cauchy stress σ_{ij} and the strain-rate potential coefficients L_{ijkl} (that can depend on u_i, σ_{ij} as well as on the entire strain history if the material went previously plastic), the rate of displacement (the velocity) v_i due to the rate of dead surface loads $\dot{t}_i$ is such that the following functional vanishes for any kinematically admissible variations of v_i

$$J(v_i)=\int_{\Pi}\left[\frac{1}{2}L_{ijkl}\,d_{ij}\,d_{kl}+\frac{1}{2}\sigma_{ij}\,v_{m,i}\,v_{m,j}\right]d\pi-\int_{\Omega}\dot{t}_i v_i\,d\Omega, \tag{2.1}$$

where the comma denotes the spatial differentiation symbol and we assume the coefficient L_{ijkl} to be derived from the strain-rate potential W as

$$\overset{\nabla}{\sigma}_{ij}=\frac{\partial W}{\partial d_{ij}}, \qquad W=\frac{1}{2}L_{ijkl}\,d_{ij}\,d_{kl}, \qquad d_{ij}=\frac{1}{2}(v_{i,j}+v_{j,i}),$$

$$\overset{\nabla}{\sigma}_{ij}=\dot{\sigma}_{ij}+\sigma_{ij}v_{k,k}-\sigma_{im}v_{j,m}-\sigma_{mj}v_{i,m},$$

where $\overset{\nabla}{\sigma}_{ij}$ denotes the Truesdell's stress rate.

The components of the given load rates $\dot{t}_i$ are measured with respect to the unit of a deformed area and the integrals in (2.1) are taken over the current volume π and the current area Ω, respectively.

If we now introduce the discretization assumption as(*)

$$v_i(x_k,t)=V_\alpha(t)\,\varphi_i^\alpha(x_k), \qquad \alpha=1,2,\ldots,N,$$

(*) We use the current coordinates as the position variables in accord with our Eulerian development.

where N is number of freedom degrees of the element considered and where φ_i^α is a set of interpolation functions associated with nodal points and V_α is a set of the nodal velocities, we arrive at

$$[k^{\alpha\beta}+k_G^{\alpha\beta}]\,V_\beta-\dot{R}^\alpha=0\,. \tag{2.2}$$

The small deformation elasto-plasticity stiffness matrix $k^{\alpha\beta}$ is given by

$$k^{\alpha\beta}=\frac{1}{2}\int_\pi L_{ijkl}\,\varphi^\alpha_{i,j}\,\varphi^\beta_{k,l}\,d\pi\,,$$

the so-called geometric stiffness matrix (also referred to as "initial stress" matrix) by

$$k_G^{\alpha\beta}=\frac{1}{2}\int_\pi \sigma_{ij}\,\varphi^\alpha_{m,i}\,\varphi^\beta_{m,j}\,d\pi$$

and the generalized load rate by

$$\dot{R}^\alpha=\int_\Omega \dot{t}_i\,\varphi_i^\alpha\,d\Omega\,.$$

To be more precise we write the matrix $k^{\alpha\beta}$ as

$$k^{\alpha\beta}=k_E^{\alpha\beta}+k_p^{\alpha\beta}\,,$$

where $k_E^{\alpha\beta}$ is the classical stiffness matrix of elasticity and $k_p^{\alpha\beta}$ is its correction (effectively with "minus" sign) due to plasticity effects. Without trying to characterize the solution procedures developed to date we present shortly the procedure applied in the paper rewriting (2.2) in a somewhat different form by replacing the velocity by the difference between the current displacement and that after the time Δt (*); moreover, Eq. (2.2) is referred to a system level rather than element level as

$$[K_E^{\alpha\beta}+K_p^{\alpha\beta}+K_G^{\alpha\beta}]\,\Delta U_\beta=\Delta F^\alpha$$

which can be put into the following form

$$[K_E^{\alpha\beta}+K_G^{\alpha\beta}]\,\Delta U_\beta=\Delta F^\alpha+J^\alpha,\qquad J^\alpha=-K_p^{\alpha\beta}\,\Delta U_\beta\,, \tag{2.3}$$

where ΔU_β is a set of the nodal displacements increments and ΔF^α is a set of the nodal force increments.

In Eq. (2.3) the so-called additional nodal forces J^α are defined as unbalanced forces appearing at each load step due to the difference between purely elastic and elasto-plastic behaviour. The formula (2.3) is now implemented by the following iteration procedure repeated at each load step

$$\begin{aligned}
&[K_E^{\alpha\beta}+K_G^{\alpha\beta}]\,\Delta U_\beta^{(\mathrm{I})}=\Delta F^\alpha+J^\alpha_{(\mathrm{I})}, && J^\alpha_{(\mathrm{I})}=0,\\
&[K_E^{\alpha\beta}+K_G^{\alpha\beta}]\,\Delta U_\beta^{(\mathrm{II})}=\Delta F^\alpha+J^\alpha_{(\mathrm{II})}, && J^\alpha_{(\mathrm{I})}=-\overset{(\mathrm{I})}{K_p^{\alpha\beta}}\,\Delta U_\beta^{(\mathrm{I})},\\
&\quad\vdots && \quad\vdots\\
&[K_E^{\alpha\beta}+K_G^{\alpha\beta}]\,\Delta U_\beta^{(n)}=\Delta F^\alpha+J^\alpha_{(n)}, && J^\alpha_{(n)}=-\overset{(n-1)}{K_p^{\alpha\beta}}\,\Delta U_\beta^{(n-1)}
\end{aligned} \tag{2.4}$$

(*) Since the loads are applied quasistatically, inertia forces may be neglected and arbitrary time scale may be chosen so that the velocities and displacement increments have the same values.

which, if converges, must be continued until the nodal forces attain constant (true) value. We stress the fact, that the current total stiffness $K_E^{\alpha\beta}+K_G^{\alpha\beta}$ of the system must be inverted at each load step resulting in highly time-consuming calculations. In spite of that we have found this method to be profitable in the case of significant nonlinearities.

Now we are to specify the above theory to the cases of truss and plane stress triangular elements.

Truss element. We define a truss as a structure which consists of a given configuration of bars connected to each other and to fixed or movable supports with perfectly hinged joints, and subjected to loads only at the connections. Each bar is of uniform cross-section and uniform properties along its length, but may differ arbitrary from other bars. The definition given above includes both the typical truss-type structures with members subjected to both extension and compression as well as prestressed networks of cables like tent roofs. The application of the present algorithm to the former case is, however, to some extent limited as the analysis of local instabilities in compression is so far not included in computer program.

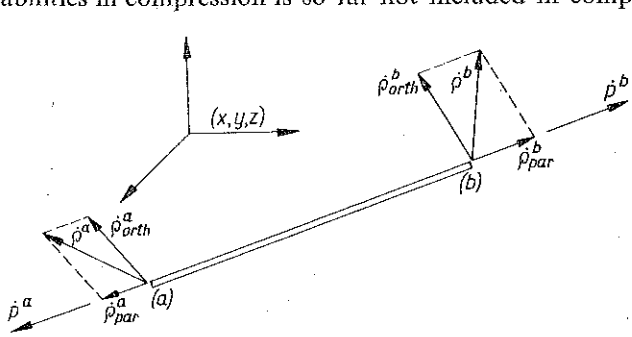

FIG. 1.

Fig. 1 introduces the notation. We confine ourselves to the considerations concerning one element only since the global stiffness matrix is built from the elemental stiffness matrices in a standard fashion.

The position of a member element in space is represented by a column vector

$$\mathbf{x}=\{x^a, y^a, z^a, x^b, y^b, z^b\} \quad \text{in which} \quad \{x^a, y^a, z^a\} \quad \text{and} \quad \{x^b, y^b, z^b\}$$

are the Cartesian coordinates of the nodal points a and b, respectively. The displacement vector of the member and its increment are given by

$$\boldsymbol{\rho}_{6\times 1}=\{\rho_x^a, \rho_y^a, \rho_z^a, \rho_x^b, \rho_y^b, \rho_z^b\}=\{\boldsymbol{\rho}^a\ \boldsymbol{\rho}^b\},$$
$$\dot{\boldsymbol{\rho}}_{6\times 1}=\{\dot{\rho}_x^a, \dot{\rho}_y^a, \dot{\rho}_z^a, \dot{\rho}_x^b, \dot{\rho}_y^b, \dot{\rho}_z^b\}=\{\dot{\boldsymbol{\rho}}^a\ \dot{\boldsymbol{\rho}}^b\},$$

while the coresponding force vector and its increment by

$$\mathbf{R}_{6\times 1}=\{R_x^a, R_y^a, R_z^a, R_x^b, R_y^b, R_z^b\}=\{\mathbf{R}^a\ \mathbf{R}^b\},$$
$$\dot{\mathbf{R}}_{6\times 1}=\{\dot{R}_x^a, \dot{R}_y^a, \dot{R}_z^a, \dot{R}_x^b, \dot{R}_y^b, \dot{R}_z^b\}=\{\dot{\mathbf{R}}^a\ \dot{\mathbf{R}}^b\}.$$

with the analogous meaning of the particular components. Direction of the member is characterized by

$$\mathbf{c}_{3\times 1}=\begin{Bmatrix} c_x \\ c_y \\ c_z \end{Bmatrix}=\frac{1}{l}\begin{Bmatrix} x^b-x^a \\ y^b-y^a \\ z^b-z^a \end{Bmatrix}.$$

We note the following group of formulae to be hold

$$\begin{aligned}
&\dot{\rho}^b_{\text{par}}=[\mathbf{c}\,\mathbf{c}^T]\,\dot{\rho}^b, \qquad \dot{\rho}_{nn}=\frac{\dot{\rho}^b_{\text{par}}-\dot{\rho}^a_{\text{par}}}{l}=\frac{1}{l}\mathbf{c}\mathbf{c}^T\{\dot{\rho}^b-\dot{\rho}^a\},\\
&\dot{\rho}^a_{\text{par}}=[\mathbf{c}\mathbf{c}^T]\,\dot{\rho}^a,\\
&\dot{\rho}^b_{\text{orth}}=[\mathbf{I}_3-\mathbf{c}\mathbf{c}^T]\,\dot{\rho}^b, \qquad \dot{\rho}_{m,\,n}=\frac{\dot{\rho}^b_{\text{orth}}-\dot{\rho}^a_{\text{orth}}}{l}=\frac{1}{l}(\mathbf{I}_3-\mathbf{c}\mathbf{c}^T)\{\dot{\rho}^b-\dot{\rho}^a\},\\
&\dot{\rho}^a_{\text{orth}}=[\mathbf{I}_3-\mathbf{c}\mathbf{c}^T]\,\dot{\rho}^a,\\
&\dot{\rho}^b-\dot{\rho}^a=[-\mathbf{I}_3\,\mathbf{I}_3]\,\dot{\rho},
\end{aligned} \tag{2.5}$$

$$\dot{\rho}_{n,\,n}=\frac{1}{l}[-\mathbf{c}\mathbf{c}^T\,\mathbf{c}\mathbf{c}^T]\,\dot{\rho},$$

$$\dot{\rho}_{m,\,n}=\frac{1}{l}[-(\mathbf{I}_3-\mathbf{c}\mathbf{c}^T)\,\mathbf{I}_3-\mathbf{c}\mathbf{c}^T]\,\dot{\rho},$$

$$\mathbf{R}=[-\mathbf{c}^T\,\mathbf{c}^T]\,\mathbf{R}_n.$$

We now specify the functional (2.1) for one-dimensional case of a bar element performing the calculation in a convective set of ccordinates rather than in a fixed one. We get from Eqs. (2.1) and (2.5)

$$J=\frac{1}{2}Al[k_{N1}\,|\dot{\rho}_{n,\,n}|^2+\sigma_{n,\,n}(|\dot{\rho}_{n,\,n}|^2+|\dot{\rho}_{m,\,n}|^2)]-\dot{\rho}^T\dot{\mathbf{R}}, \tag{2.6}$$

where A is the cross-section and l — the length of a bar, and where σ_{nn} stands for the only component of the stress state and k_{N1} is the natural stiffness of the element to be specified. We assume further the stress component σ_{nn} to be negligible in comparison to the siffness k_{N1} (what is the case for metals).

The functional (2.6) takes the form

$$J(\dot{\rho})=\frac{1}{2}Al[k_{N1}\,|\dot{\rho}_{n,\,n}|^2+\sigma_{nn}\,|\dot{\rho}_{m,\,n}|^2]-\dot{\rho}^T\dot{\mathbf{R}}$$

or, on using (2.5), the form

$$\begin{aligned}
J(\dot{\rho})=\frac{1}{2}\,\frac{A}{l}\{&\dot{\rho}^T[-\mathbf{c}\mathbf{c}^T\,\mathbf{c}\mathbf{c}^T]^T k_{N1}\,[-\mathbf{c}\mathbf{c}^T\,\mathbf{c}\mathbf{c}^T]\,\dot{\rho}+\\
&+\dot{\rho}^T[-(\mathbf{I}_3-\mathbf{c}\mathbf{c}^T)\,\mathbf{I}_3-\mathbf{c}\mathbf{c}^T]\,\sigma_{nn}\,[-(\mathbf{I}_3-\mathbf{c}\mathbf{c}^T)\,\mathbf{I}_3-\mathbf{c}\mathbf{c}^T]\,\dot{\rho}\}-\dot{\rho}^T\dot{\mathbf{R}}.
\end{aligned} \tag{2.7}$$

If we now minimize the functional (2.7) by considering $\delta J=\dfrac{\partial J}{\partial\dot{\rho}}\,\delta\dot{\rho}=0$ we shall arrive at

$$\frac{Ak_{N1}}{l}\begin{bmatrix} \mathbf{c}\mathbf{c}^T & -\mathbf{c}\mathbf{c}^T \\ -\mathbf{c}\mathbf{c}^T & \mathbf{c}\mathbf{c}^T \end{bmatrix}\dot{\rho}+\frac{R_n}{l}\begin{bmatrix} \mathbf{I}_3-\mathbf{c}\mathbf{c}^T & -(I_3-\mathbf{c}\mathbf{c}^T) \\ -(\mathbf{I}_3-\mathbf{c}\mathbf{c}^T) & \mathbf{I}_3-\mathbf{c}\mathbf{c}^T \end{bmatrix}\dot{\rho}=\dot{\mathbf{R}}$$

or, shorter, at

$$[\mathbf{k}_{E-P,1}+\mathbf{k}_{G,1}]\dot{\boldsymbol{\rho}}=\dot{\mathbf{R}}, \tag{2.8}$$

in which the elasto-plastic stiffness matrix $k_{E-P,1}$ is seen to be

$$\mathbf{k}_{E-P,1}=\frac{k_{N1}A}{l}\begin{bmatrix}\mathbf{cc}^T & -\mathbf{cc}^T\\ -\mathbf{cc}^T & \mathbf{cc}^T\end{bmatrix}$$

while the geometric stiffness matrix $\mathbf{k}_{G,1}$

$$\mathbf{k}_{G,1}=\frac{R_n}{l}\begin{bmatrix}\mathbf{I}_3-\mathbf{cc}^T & -(\mathbf{I}_3-\mathbf{cc}^T)\\ -(\mathbf{I}_3-\mathbf{cc}^T) & \mathbf{I}_3-\mathbf{cc}^T\end{bmatrix}.$$

From (2.8) the total stiffness matrix can be assambled in a common manner. We note that the incremental stiffness matrices presented herein are equivalent to those derived for elastic trusses in [8].

Triangular plane stress element. In the development of a triangular plane stress element it is assumed that the element lies in the x-y plane as shown in Fig. 2. The element (a)–(b)–(c) of arbitrary triangular shape is located arbitrarily in relation

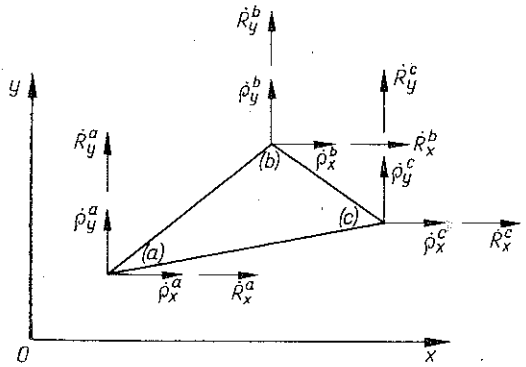

FIG. 2.

to a rectangular coordinate system (x, y). The velocites (the displacement increments) of an arbitrary point are denoted by v_x, v_y ($\Delta u_x, \Delta u_y$) and the nodal velocites $\dot{\rho}_x, \dot{\rho}_y$ are indexed according to the nodal description.

The following presentation of the conventional matrix is to a large extent in accordance with the classical development of [9] and it is why the geometric stiffness matrix only will be described here in some details.

If we express v_x and v_y as the first degree polynomials in x and y, then we get

$$v_x(x,y)=\frac{1}{2\Omega}[1xy]\mathbf{A}\mathbf{V}_x, \qquad v_y(x,y)=\frac{1}{2\Omega}[1xy]\mathbf{A}\mathbf{V}_y,$$

where Ω is the area of the triangle and

$$\mathbf{V}_x=\begin{Bmatrix}\dot{\rho}_x^a\\ \dot{\rho}_x^b\\ \dot{\rho}_x^c\end{Bmatrix},\qquad \mathbf{V}_y=\begin{Bmatrix}\dot{\rho}_y^a\\ \dot{\rho}_y^b\\ \dot{\rho}_y^c\end{Bmatrix},$$

$$\mathbf{A}=\begin{bmatrix}\mathbf{A}_1\\ \mathbf{A}_2\\ \mathbf{A}_3\end{bmatrix}=\begin{bmatrix}x_by_c-x_cy_b & x_cy_a-x_ay_c & x_ay_b-x_by_a\\ y_b-y_c & y_c-y_a & y_a-y_b\\ x_c-x_b & x_a-x_c & x_b-x_a\end{bmatrix}.$$

We have also

$$v_{x,x}=\mathbf{A}_2\mathbf{V}_x,\qquad v_{y,x}=\mathbf{A}_2\mathbf{V}_y,$$

$$v_{x,y}=\mathbf{A}_3\mathbf{V}_x,\qquad v_{y,y}=\mathbf{A}_3\mathbf{V}_y.$$

The functional (2.1) for the plane stress case takes the form

$$J(\mathbf{v})=\int_\Omega\left(\frac{1}{2}L_{\alpha\beta\gamma\delta}\,d_{\alpha\beta}\,d_{\gamma\delta}+\frac{1}{2}\sigma_{\alpha\beta}v_{\delta,\alpha}v_{\gamma,\beta}\right)d\Omega-\dot{\mathbf{R}}^T\mathbf{V}, \tag{2.9}$$

where

$$\mathbf{V}=\begin{Bmatrix}\mathbf{V}_x\\ \mathbf{V}_y\end{Bmatrix},\qquad \dot{\mathbf{R}}=\begin{Bmatrix}\dot{\mathbf{R}}_x\\ \dot{\mathbf{R}}_y\end{Bmatrix},\qquad \dot{\mathbf{R}}_x=\begin{Bmatrix}\dot{\mathbf{R}}_x^a\\ \dot{\mathbf{R}}_x^b\\ \dot{\mathbf{R}}_x^c\end{Bmatrix},\qquad \dot{\mathbf{R}}_y=\begin{Bmatrix}\dot{\mathbf{R}}_y^a\\ \dot{\mathbf{R}}_y^b\\ \dot{\mathbf{R}}_y^c\end{Bmatrix}.$$

The first part of (2.9) gives rise to the classical Cartesian stiffness matrix of the infinitesimal deformation problem and therefore will not be further written out in full.

If we denote

$$\mathbf{V}_x=\mathbf{\Lambda}_x\mathbf{V},\qquad \mathbf{V}_y=\mathbf{\Lambda}_y\mathbf{V},$$

$$\mathbf{\Lambda}_x=[\mathbf{I}_3\,\mathbf{O}_3].\qquad \mathbf{\Lambda}_y=[\mathbf{O}_3\,\mathbf{I}_3],$$

the functional (2.9) can be rewritten as

$$J(\mathbf{V})=\frac{1}{2}\int_\Omega\mathbf{V}^T\mathbf{k}_{E-P,2}\,\mathbf{V}d\Omega+\frac{1}{2}\int_\Omega\mathbf{V}^T\mathbf{k}_{G,2}\,\mathbf{V}d\Omega-\dot{\mathbf{R}}^T\mathbf{V}, \tag{2.10}$$

where the geometric stiffness matrix $\mathbf{k}_{G,2}$ is given by

$$\mathbf{k}_{G,2}=\sigma_{11}(\mathbf{\Lambda}_x^T\mathbf{A}_3^T\mathbf{A}_3\mathbf{\Lambda}_x+\mathbf{\Lambda}_y^T\mathbf{A}_3\mathbf{A}_3\mathbf{\Lambda}_y)+\sigma_{12}(\mathbf{\Lambda}_x^T\mathbf{A}_3^T\mathbf{A}_2\mathbf{\Lambda}_x+\mathbf{\Lambda}_y^T\mathbf{A}_3^T\mathbf{A}_2\mathbf{\Lambda}_y)+$$
$$+\sigma_{22}(\mathbf{\Lambda}_x^T\mathbf{A}_2^T\mathbf{A}_2\mathbf{\Lambda}_x+\mathbf{\Lambda}_y^T\mathbf{A}_2^T\mathbf{A}_2\mathbf{\Lambda}_y).$$

On minimizing the functional (2.10) with respect to the velocity field we get

$$[\mathbf{k}_{E-P,2}+\mathbf{k}_{G,2}]\,\mathbf{V}=\dot{\mathbf{R}}.$$

As before, referring to the standard procedures for assembling the structure matrices, there is no need to consider the derivation of the matrices for more than one single element.

3. Description of the computer program

The calculations have been based on the subroutines of the ASKA program package available at the Institut für Statik u. Dynamik der Luft-u. Raumfahrtkonstruktionen. The computational steps and other important features of the program as adapted by the authors are as follows, cf. Fig. 3:

1. Reading input data which consist of parameters defining the type problem to be solved, such as the type of element TRIM 3 — constant strain triangle for plane stress analysis, FLA 2 — one-dimensional truss element in three-dimensional space, material data (elasticity or elasto-plasticity), nodal point coordinates, boundary conditions, i.e., prescribed forces and/or prescribed displacements, total value of the generalized loading, number of the load steps in the incremental analysis and their magnitude, parameters of the iteration procedure, output requirements.

2. First linear elastic step of the incremental solution needed for some program organization purposes.

3. Next step of the incremental solution. Updating of the geometry of the formation of the new stiffness matrix.

Iteration loop for plasticity based on the "initial load" technique composed of: a) estimation of the equivalent plastic strain increment; b) calculation of the elemental initial load increments; c) calculation of the total load increment of the structure; d) calculation of the displacement increment by a forward and back-substitution on the right-hand side of the fundamental stiffness equation at the load step considered. The actual stiffness matrix has been decomposed at the beginning of the current load steps; e) calculation of the stress increments and, by accumulation (hyper-matrix addition), calculation of the current value of stresses; f) calculation of the equivalent plastic strain increments.

The next iteration step is executed and the cyclic procedure is repeated until the successive equivalent plastic strain increments become sufficiently close. We proceed then to the next load increment.

In numerical examples, the analysis in the plastic range of deformation has been based on the isotropic work-hardening assumptions and stress-strain law represented in uniaxial case by a modified Ramberg-Osgood relation of the form

$$\eta_p = \frac{1.1\,\sigma_{pl_0}}{mE}\left[\left(\frac{\sigma}{1.1\,\sigma_{pl_0}}\right)^m - \left(\frac{1}{1.1}\right)^m\right],$$

where η_p is plastic strain, which, for some material parameters E, yield stress σ_{pl_0} and exponent m, properly characterizes the strain hardening of the alluminium alloy. Other hardening theories have been also tested.

4. Examples

In order to illustrate the above method for solving elasto-plastic problems in the geometrically nonlinear range of deformation we start with an example of the analysis of a truss as shown in Fig. 4. In the first part of the analysis the proportionally

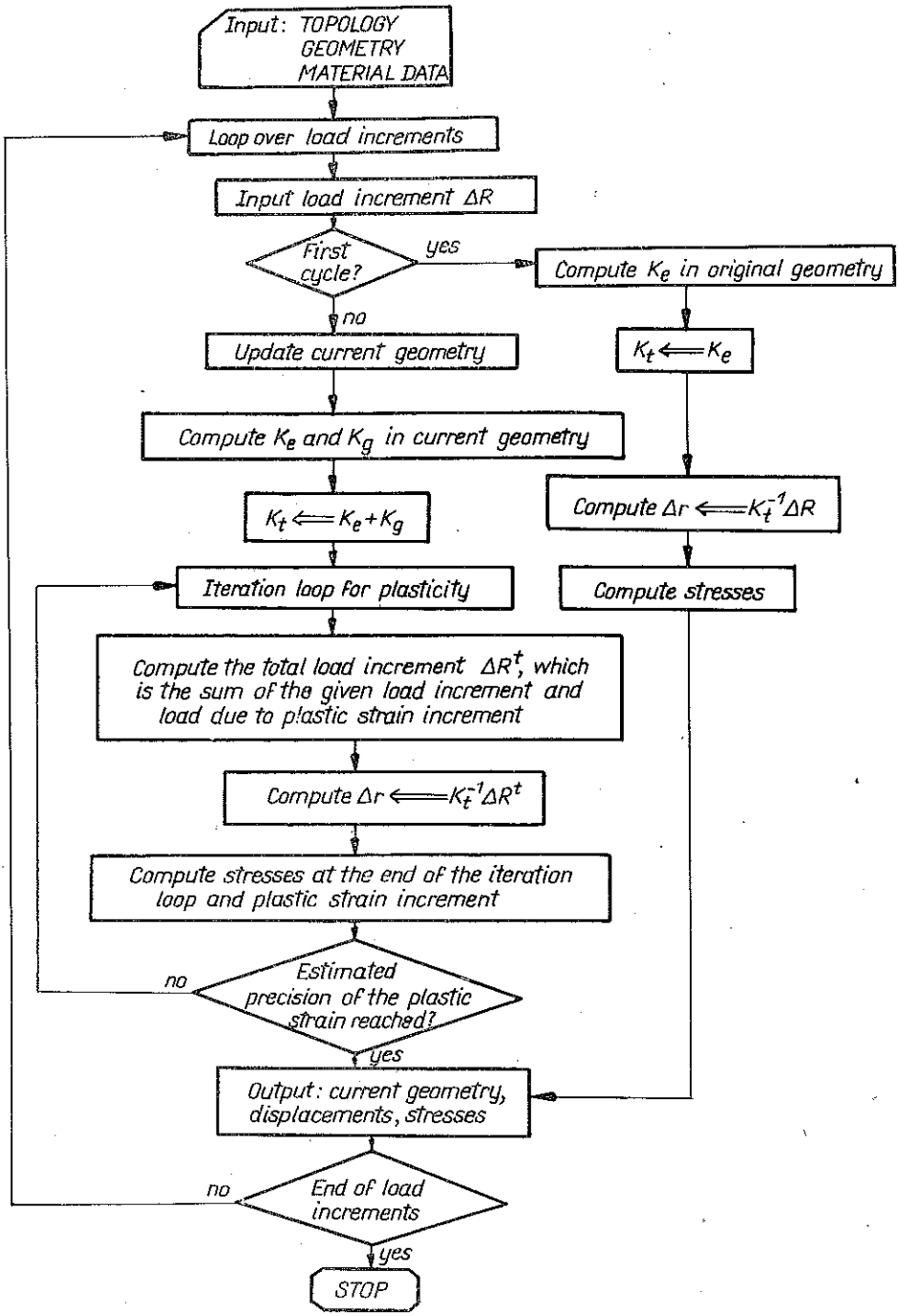
Input: TOPOLOGY
GEOMETRY
MATERIAL DATA
Loop over load increments
Input load increment ΔR
First cycle?
yes
no
Compute K_e in original geometry
Update current geometry
$K_t \Longleftarrow K_e$
Compute K_e and K_g in current geometry
$K_t \Longleftarrow K_e + K_g$
Compute $\Delta r \Longleftarrow K_t^{-1} \Delta R$
Iteration loop for plasticity
Compute stresses
Compute the total load increment ΔR^t, which is the sum of the given load increment and load due to plastic strain increment
Compute $\Delta r \Longleftarrow K_t^{-1} \Delta R^t$
Compute stresses at the end of the iteration loop and plastic strain increment
Estimated precision of the plastic strain reached?
no
yes
Output: current geometry, displacements, stresses
End of load increments
no
yes
STOP

FIG. 3.

increasing (from 0 to P_{end}) forces were applied to the truss. The analysis was repeated four times for four different load steps (Table 1), leading to the results given in Table 2. For some chosen values of the current loading the greatest vertical dis-

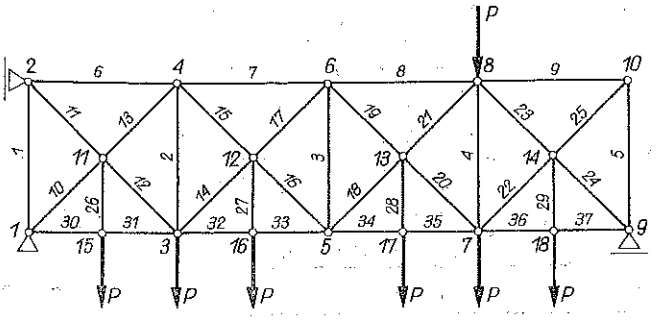

FIG. 4.

placement (of the node 17) related to the height of the truss is given as well as the relative elongation of the bar 37 (ε_{37}) and the relative stress in the bar 12 (σ_{pl_0} is initial yield value). For comparison purposes the displacement of the node 17 and stress in the bar 12 are also given as calculated under the assumption of the geometrically linear behaviour of the truss.

Table 1.

Number of loading path	I	II	III	IV
Number of increments	43	22	15	8
First increment			$.276P_{end}$	
Next increments	$.01724P_{end}$	$.03448P_{end}$	$.05171P_{end}$	$.09050P_{end}$
Final load		P_{end}		
Time of calculation	100%	38%	50%	42%

The results indicate clearly, that up to the displacement of the order of 30% of the characteristic truss dimension the results obtained as a function of a steps number differ not more than 1% in the case of the displacements and not more than 2% in the case of stresses. For the greater displacements of the practically unrealistic order those differences reach the level of 15%. We note that the smallest amount of the time was needed for the analysis with 22 increments of load.

The next comparison concerns once more the difference between the solutions obtained within the geometrically linear and nonlinear theories, Figs. 5, 6. The stress distribution shown in Fig. 6 indicates the danger of omitting some important features of the structure behaviour if the change in geometry is not included — the unloading phenomenon proved to be only a result of geometric nonlinearities. Fig. 7 shows additionally the subsequent phases of the process.

Table 2.

	Geometric nonlinearity												Geometric linearity	
	$\lvert u_{17}/h \rvert$				ε_{37}				$\sigma_{12}/\sigma_{pl_0}$				$\lvert u_{17}/h \rvert$	$\sigma_{12}/\sigma_{pl_0}$
P/P_{end}	I	II	III	IV	I	II	III	IV	I	II	III	IV		
.2759	.0108	.0108	.0108	.0108	.00148	.00148	.00148	.00148	.5674	.5675	.5675	.5675	.0108	.5675
.3793	.0151	.0151	.0151	.0151	.00203	.00203	.00203	.00203	.8079	.8079	.8081	.8083	.0151	.8084
.4828	.0233	.0233	.0233	.0233	.00258	.00258	.00258	.00260	1.0668	1.0632	1.1701	1.1771	.0231	1.0771
.5868	.0531	0.532	.0533	.0535	.00321	.00327	.00332	.00336	1.2489	1.2334	1.2449	1.2502	.0506	1.3161
.6897	.1387	.1529	.1614	.1701	.00568	.00661	.00741	.00801	1.3036	1.2909	1.3080	1.2980	.1260	1.5516
.7931	.3162	.3112	.3201	.3198	.01972	.01841	.01946	.01912	1.1902	1.1877	1.1653	1.1600	.2476	1.7826
.8966	.5478	.5050	.5047	.4918	.06041	.04603	.04347	.03917	.8470	.9732	.9033	.9912	.3888	2.0037
1.0	.8524	.7243	.7160	.6771	.18980	.09474	.08952	.06690	.7591	.7417	.7037	.6437	.4566	2.2165

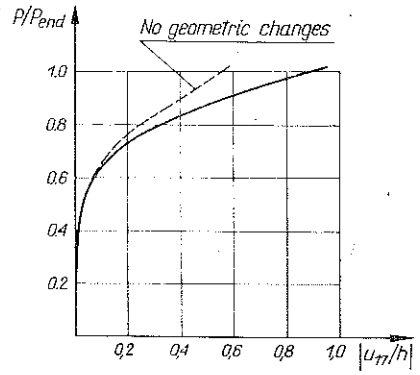

FIG. 5.

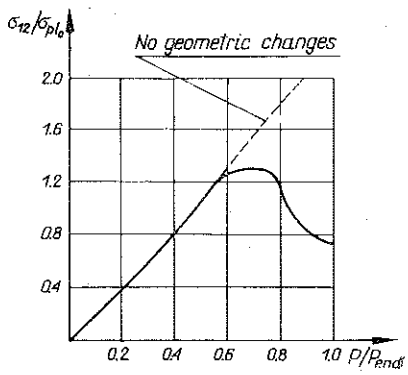

FIG. 6.

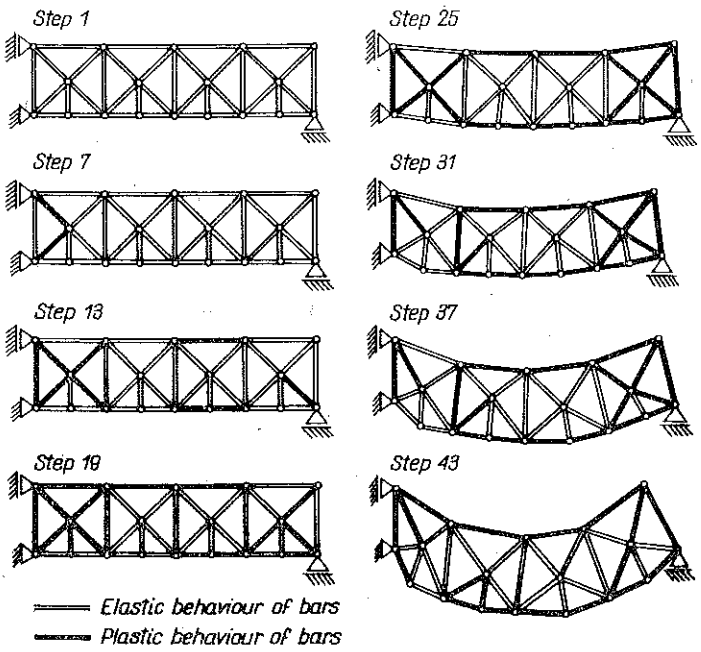

FIG. 7.

As the next step we attempted to investigate the influence of the load history on the final state of the truss. This analysis has been illustrated in Table 3 and in Fig. 9 for the optimal version of the 22 steps-incremental analysis. The history of the load is shown in Fig. 8.

As the next example of large deformation, elasto-plastic analysis the plane stress problem of a perforated plate with a ratio of hole diameter to plate width of 1/2 was considered. The plate was subjected to uniformly distributed loading of intensity σ_{ext}. The plate, its dimensions and properties are shown in Fig. 10. The next Fig. 11 presents the finite element mesh and the boundary conditions for the quarter of the plate which was analysed. The 20 loading steps were applied.

Table 3.

Case of the load history	I			II			III		
Load step	P/P_{end}	$\lvert u_{17}/h\rvert$	$\sigma_{12}/\sigma_{pl_0}$	P/P_{end}	$\lvert u_{17}/h\rvert$	$\sigma_{12}/\sigma_{pl_0}$	P/P_{end}	$\lvert u_{17}/h\rvert$	$\sigma_{12}/\sigma_{pl_0}$
1	.2759	.0108	0.5675	.2759	.0108	0.5675	.2759	.0108	0.5675
4	.3690	.0141	0.8498	.40	.0170	0.8248	.3571	.0133	0.8669
7	.4621	0.246	1.0537	.5241	0.319	1.1110	.4384	.0277	1.0268
10	.5552	.0634	1.1491	.6483	.0955	1.4347	.5197	.0860	1.1108
13	.6614	.1496	1.1549	.7461	.2577	1.5172	.6292	.1743	1.0976
16	.7743	.2603	1.0929	.8307	.5538	1.1198	.7528	.2868	0.9926
19	.8872	.4295	0.9073	.9154	.8877	.09761	.8764	.4572	0.7413
22	1.0	.7820	0.6613	1.0	1.4444	1.0823	1.0	.8824	0.6273

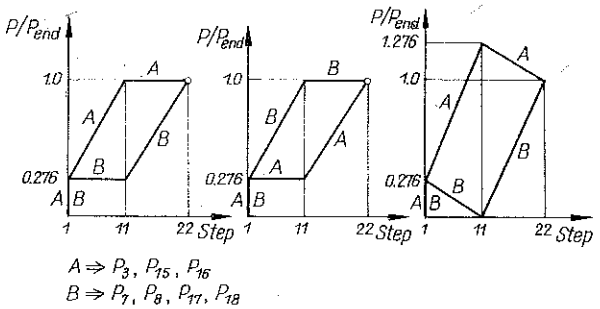

FIG. 8.

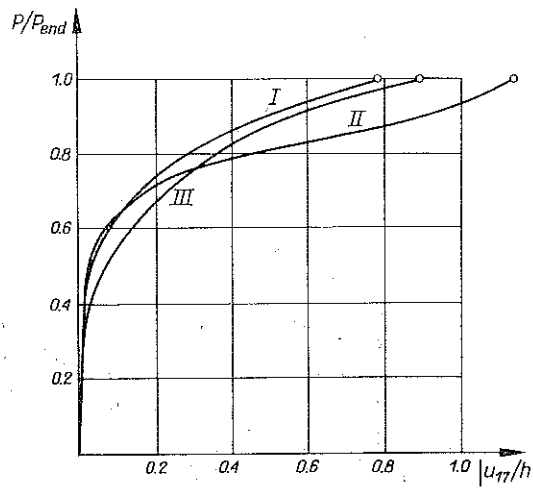

FIG. 9.

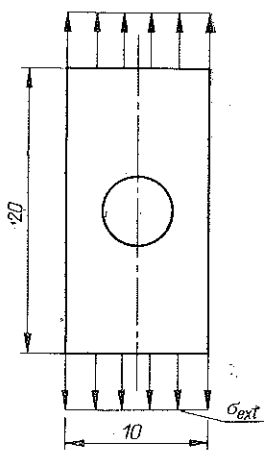

FIG. 10.

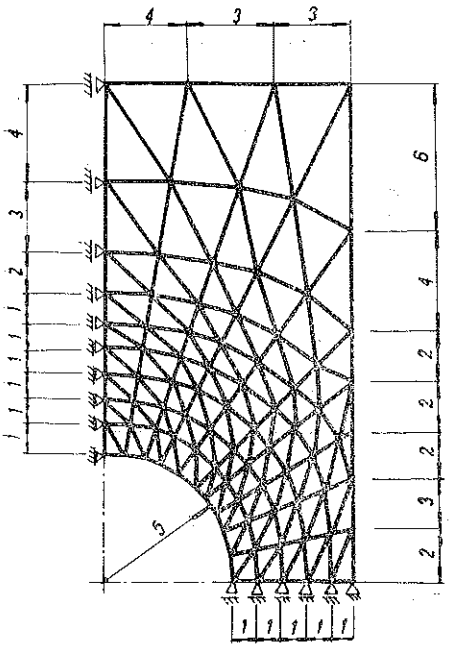

FIG. 11.

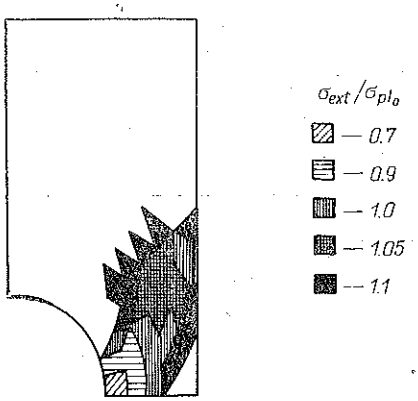

FIG. 12.

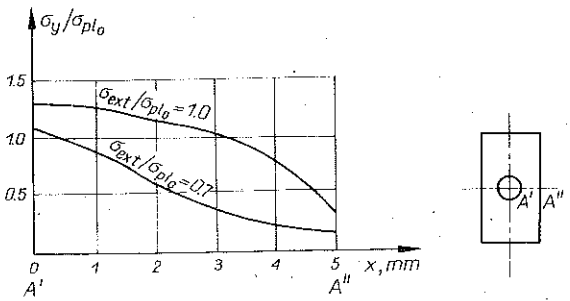

FIG. 13.

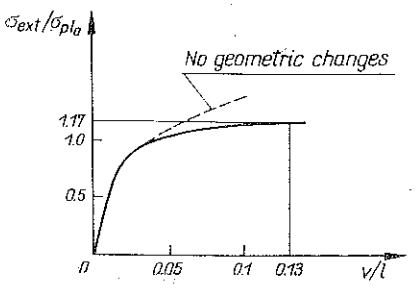

FIG. 14.

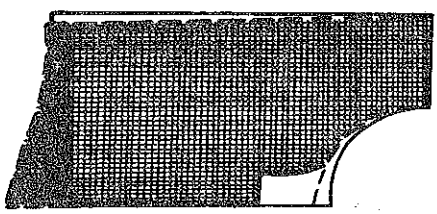

FIG. 15.

The plastic zones for various loads are shown in Fig. 12. That figure and all others are scaled with regard to the yield stress σ_{pl_0}. The first element went plastic at value of the external stress equal to $0.7\sigma_{pl_0}$. A plot of the longitudinal stress distribution σ_y at the smallest cross-section of the plate for $\sigma_{ext}/\sigma_{pl_0}=1.0$ and $\sigma_{ext}/\sigma_{pl_0}=0.7$ is shown in Fig. 13. The next figure shows the relation stress against the relative displacement of the point A' during the deformation process. It has been observed that for the value of $\sigma_{ext}/\sigma_{pl_0}=1.17$ the peak load occurs as the resulting set of equations becomes unstable. The analysis could be then continued only under geometric external loading but that was not attempted by the authors. Such a furtherance of the analysis, however, would be every interesting. The plastic region continued to grow until almost all of the quadrant has yielded except for a small region located above the void, cf. Fig. 15. No unloading regions have been observed. The analysis had been terminated at the significant geometry changes (Fig. 14), which suggests that the geometrically linear analysis would be insufficient. In fact, cf. Fig. 14, the stress-elongation curve for such a case differs significantly from that for geometrically nonlinear analysis and, basides, the peak load has not been observed.

5. Conclusions

The approach to the derivations of the fundamental equations of the finite element method via the varitional principle presented above makes it possible to get all the matrices of the problem in a clear and elegant form.

The methods enables the geometrically nonlinear problems to be solved using the ASKA progam package for physically nonlinear analysis without an interference with its internal structure. The algorithm has been built basing upon the updating of the geometry and adding the geometric stiffness matrices at each load step and solving the resulting elasto-plastic problem by means of the standard iterative procedure.

Within the class of the problems considered that is apart from the stability analysis, the number of the "geometry corrections" has not significantly influenced the final results. However, the differences in the computer time as well as the differences between the geometrically linear and nonlinear approach can be of a great significance. The optimal number of the load increments should be always carefully sought but care must also be taken as that number is strongly dependent on the algorithm to be used in calculations.

The analysis could be much more effective if the calculations were performed within the system designed specially from the very beginning as the system to account for geometrically nonlinear effects.

References

1. C. A. Felippa, *Refined finite analysis of linear and nonlinear two-dimensional structure*, SESM 66-22, University of Calif., Oct. 1966.
2. P. V. Marcal, *Large deflection analysis of elastic-plastic shells of revolution*, AISSI ASME 10th Conference, New Orleans, April 1969.

3. S. YAGHMAI, *Incremental analysis of large deformation in mechanics of solids with application to axisymmetric shells of revolution*, SESM 68-17, University of Calif., Dec. 1968.
4. H. D. HABBIT, P. V. MARCAL, J. R. RICE, *A finite element formulation for problems of large strain and large displacement*, Int. J. Sol. Struct., **6**, 1970.
5. J. A. STRICKLIN, W. E. HAISLER, W.A. VON RIESEMANN, *Computation and solution procedures for nonlinear analysis by combined finite element — finite difference methods*, Comp. Struct., **2**, 1972.
6. H. LEVINE, H. ARMEN, Jr., R. WINTER, *Theoretical and experimental investigation of the large deflection, elastic-plastic behaviour of orthotropic shells of revolution under cyclic loading*, Nat. Symp. G. Washington Univ., Washington D. C., March 1972.
7. M. KLEIBER, *Lagrangian and Eulerian finite element foruulation for large strain elasto-plasticity*, Bull. Acad. Polon. Sci., Série Sci. Techn., **23**, 3, 1975.
8. J. H. ARGYRIS, D. W. SCHARF, *Large deflection analysis of prestressed networks*, J. Struct. Div., **98**, 3, 1972.
9. R. W. CLOUGH, *The finite element method in structural mechanics, Stress Analysis*, J. Wiley and Sons Ltd., London–New York–Sydney 1965.

STRESZCZENIE

ANALIZA GEOMETRYCZNIE I FIZYCZNIE NIELINIOWYCH KONSTRUKCJI METODĄ JEDNO I DWUWYMIAROWYCH ELEMENTÓW SKOŃCZONYCH

W pracy rozpatrzono rozwiązanie problemu dużych odkształceń elasto-plastycznych metodą elementów skończonych. Na podstawie twierdzenia wariacyjnego wyprowadzono podstawowe równania metody przyrostowej we współrzędnych Eulera oraz omówiono szczegółowo wyznaczanie geometrycznej macierzy sztywności dla geometrycznie nieliniowych, jedno- i dwuwymiarowych zagadnień. Omówiono ponadto zastosowany program obliczeń, oparty na systemie ASKA. Pracę zilustrowano przykładami numerycznymi.

Резюме

АНАЛИЗ ГЕОМЕТРИЧЕСКИЙ И ФИЗИЧЕСКИЙ НЕЛИНЕЙНЫХ КОНСТРУКЦИЙ МЕТОДОМ ОДНО- И ДВУХМЕРНЫХ КОНЕЧНЫХ ЭЛЕМЕНТОВ

В работе рассмотрено решение задачи больших упруго-пластических деформаций методом конечных элементов. Опираясь на вариационную теорему выведены основные уравнения метода в приростах в Эйлеровых координатах, а также обсуждено подробно определение геометрической матрицы жесткости для геометрически нелинейных одно- и двухмерных задач. Кроме этого обсуждена применяемая программа расчетов, опирающаяся на систему АСКА. Работу иллюстрируют численные примеры.

Received February 19, 1976.